

Generation of arbitrary full Poincaré beams on the hybrid-order Poincaré sphere

Xiaohui Ling,^{1,2,*} Xunong Yi¹, Zhiping Dai², Youwen Wang², and Liezun Chen²

¹*SZU-NUS Collaborative Innovation Center for Optoelectronic Science and Technology,*

and Key Laboratory of Optoelectronic Devices and Systems

of Ministry of Education and Guangdong Province,

College of Optoelectronic Engineering,

Shenzhen University,

Shenzhen 518060, China

²*Laboratory for Optics and Optoelectronics,*

Department of Physics and Electronic Information Science,

Hengyang Normal University,

Hengyang 421002, China

(Dated: September 13, 2018)

Abstract

We propose that the full Poincaré beam with any polarization geometries can be pictorially described by the hybrid-order Poincaré sphere whose eigenstates are defined as a fundamental-mode Gaussian beam and a Laguerre-Gauss beam. A robust and efficient Sagnac interferometer is established to generate any desired full Poincaré beam on the hybrid-order Poincaré sphere, via modulating the incident state of polarization. Our research may provide an alternative way for describing the full Poincaré beam and an effective method to manipulate the polarization of light.

*Electronic address: xhling@hnu.edu.cn

I. INTRODUCTION

Polarization is a fundamental property of light. Conventional states of polarization, including linear, circular, and elliptical polarizations have homogeneous spatial distribution. Arbitrary polarization state can be described pictorially as a point in the surface of a unit sphere, named as Poincaré sphere [1]. In recent years, optical beams with inhomogeneous polarization in the transverse plane, such as cylindrical vector beam, have drawn much attention due to its intriguing properties under high-numerical-aperture focusing and a range of potential applications, such as in optical trapping, high-resolution metrology, and electron acceleration [2, 3]. This kind of beams can be represented by higher-order Poincaré spheres [4, 5]. In fact, optical beams can simultaneously exhibit inhomogeneous polarization and phase, such as cylindrical vector vortex beams [6–10]. Apart from the inhomogeneous polarization, the vector vortex beams have a helical (vortex) phase factor. We have generalized the fundamental Poincaré sphere to a hybrid-order Poincaré sphere to describe the vector vortex beams[11]. Recently, a new class of beam with inhomogeneous polarization distribution, full Poincaré beam (FPB), which covers all possible polarization states over the fundamental Poincaré sphere in its transverse plane, has been proposed [12, 13]. It can be generated by coaxial superposition of a fundamental-mode Gaussian beam and a Laguerre-Gauss beam [12–15] or untuned q-plates [16, 17]. The FPBs exhibit polarization singularities and therefore have great potential in the singular optics [16–20]. In addition, the FPBs can be used for beam shaping [14] or studying the geometric Pancharatnam-Berry in optical system [21, 22].

In this paper, we propose that the FPB can be pictorially described by the hybrid-order Poincaré sphere which is established by defining the orthogonal eigenstates with a fundamental Gaussian beam and a Laguerre-Gauss beam. A Sagnac interferometer is employed to generate the FPB. The setup composed of a spatial light modulator, a polarizing beam splitter, and a mirror. The setup converts the horizontal polarization light into a vortex-bearing beam and remains the vertical one unchanged. Their coaxial superposition manifests as a FPBs. Controlling the incident polarization with a polarizer and a quarter-wave plate, we can realize arbitrary FPBs on the hybrid-order Poincaré sphere.

II. HYBRID-ORDER POINCARÉ SPHERE

The fundamental Poincaré sphere can represent all the conventional states of polarization, linear, circular, and elliptical. The north and south poles correspond to the left- and right-handed

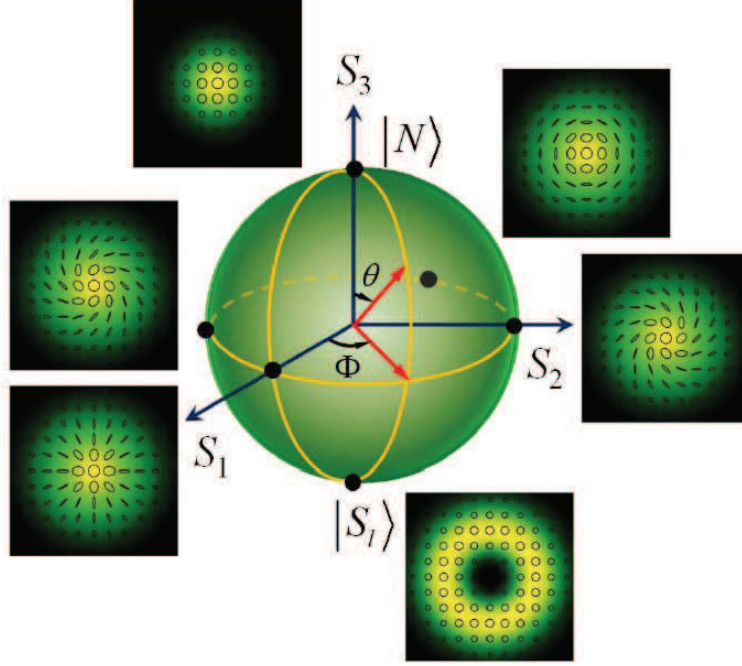


FIG. 1: Schematic of the hybrid-order Poincaré sphere for $l = 2$. The insets indicate the intensity background and polarization geometries (ellipses) of six FPBs on the equator and poles, respectively.

circular polarization (eigenstates), respectively. Their equal-weight superposition results in the states of polarization on the equator, i.e., linear polarizations. Others located between the poles and the equator, are elliptical polarizations. While the orthogonal eigenstates of the hybrid-order Poincaré sphere are defined as two circular polarizations with different vortex phase factors, and they can synthesise the vector vortex beams [11].

We here establish a hybrid-order Poincaré sphere with its orthogonal circular-polarization eigenstates being a fundamental-mode Gaussian beam and a Laguerre-Gauss beam. Suitable superposition of the eigenstates can generate any desired FPBs, and thus the proposed hybrid-order Poincaré sphere can be used to describe the FPB, i.e., any FPB corresponds to a point on the surface of the unit sphere. An alternative algebraic representation of the FPB can be written as

$$|\psi_l\rangle = \psi_N |N\rangle + \psi_S^l |S_l\rangle, \quad (1)$$

where the circular polarization eigenstates are

$$|N\rangle = \frac{1}{\sqrt{2}}(\hat{e}_x + i\hat{e}_y)\text{LG}_{0,0}, \quad |S_l\rangle = \frac{1}{\sqrt{2}}(\hat{e}_x - i\hat{e}_y)\text{LG}_{0,l}. \quad (2)$$

Here, \hat{e}_x (\hat{e}_y) is the unit vector in the x (y) direction. ψ_N and ψ_S^l are complex amplitudes of the orthogonal circular polarization bases, respectively. $\text{LG}_{0,0}(r, z)$ represents a fundamental-mode

Gaussian beam propagating in the z direction with $r = (x^2 + y^2)^{1/2}$ being the transverse coordinate, which can be expressed as

$$\text{LG}_{0,0}(r, z) = A_0 \frac{w_0}{w(z)} \exp\left[-\frac{r^2}{w^2(z)}\right] \exp\left[-i\left(kz - \frac{kr^2}{2R(z)} - \xi(z)\right)\right], \quad (3)$$

where A_0 is a constant, k is the free-space wavevector, $w_0 = w(0)$ is the beam waist size, $R(z)$ is the radius of curvature of the beam's wavefronts, and $\xi(z) = \tan^{-1}[z/z_R]$ is the Gouy phase with $z_R = kw_0^2/2$ being the Rayleigh distance. The Laguerre-Gauss beam $\text{LG}_{0,l}$ can be expressed as

$$\text{LG}_{0,l}(r, z) = \text{LG}_{0,0}(r, z) \left[\frac{\sqrt{2}r}{w(z)}\right]^{|l|} \exp(il\varphi) \exp[i|l|\xi(z)], \quad (4)$$

where $\varphi = \arctan(y/x)$ is the azimuthal angle and l is the topological charge of the vortex phase.

The state of polarization on the hybrid-order Poincaré sphere can be defined by two independent parameters (θ, Φ) with $\theta \in [0, \pi]$ and $\Phi \in [0, 2\pi]$, which fix the colatitude and azimuthal angles on the sphere, as depicted in Fig. 1. Then we can obtain that

$$\tan\left(\frac{\theta}{2}\right) = \frac{|\psi_S^l|}{|\psi_N^l|}, \quad \Phi = \arg(\psi_S^l) - \arg(\psi_N^l). \quad (5)$$

For $\theta = 0$ and π , Equation (1) represents the FPBs on the north and south poles, respectively. When $\theta = \pi/2$, i.e., $|\psi_N^l| = |\psi_S^l|$, the FPB locates on the equator, representing the equal-intensity superposition of the two orthogonal bases. Other values of θ indicate the FPBs on the spheres between the poles and the equator. In addition, Φ defines the value of the longitude.

The sphere's Cartesian coordinates now can be represented by the Stokes parameters [1]

$$S_0 = |\psi_N^l|^2 + |\psi_S^l|^2, \quad S_1 = 2|\psi_N^l||\psi_S^l| \cos \Phi, \quad S_2 = 2|\psi_N^l||\psi_S^l| \sin \Phi, \quad S_3 = |\psi_N^l|^2 - |\psi_S^l|^2. \quad (6)$$

S_0 is unit radius of the hybrid-order Poincaré sphere and $S_{1,2,3}$ are the sphere's Cartesian coordinates. For $l = 0$, the hybrid-order Poincaré sphere reduces to the well-known fundamental Poincaré sphere. Figure 1 depicts a hybrid-order Poincaré sphere for $l = 2$, where six FPBs located on the equator and poles are given.

III. EXPERIMENTAL SCHEME

We implement an experimental setup to generate the FPBs, as depicted in Fig. 2. A Glan laser polarizer (GLP) and quarter-wave plate (QWP1) can convert the laser beam output from the He-Ne laser (operational wavelength $\lambda = 632.8$ nm and beam waist size $w_0 = 0.7$ mm) into any

desired state of polarization (linear, circular, and elliptical). Assumed the transmission axis of the GLP and optical axis of the QWP1 incline angles γ and ψ with respect to the horizontal direction, respectively, the Jones vector of the light beam after the QWP1 can be written as

$$[\cos \gamma - i \cos(2\psi - \gamma)]\text{LG}_{0,0}\hat{e}_x + [\sin \gamma - i \sin(2\psi - \gamma)]\text{LG}_{0,0}(r, z)\hat{e}_y. \quad (7)$$

Then the beam propagates into a Sagnac interferometer consisting of a polarizing beam splitter (PBS), a phase-only spatial light modulator (SLM), and a mirror (M). The PBS transmits the horizontal polarization component and reflects the vertical polarization component of the incident beam. The horizontal polarization sub-beam acquires a helical vortex phase after reflecting by the SLM and propagates anticlockwise in the interferometer, which is a good approximation of the vortex-bearing Laguerre-Gauss beam $\text{LG}_{0,l}$, expressed by Eq. (4). Note that the reflection of the mirror reverses the topological charge of the vortex from l to $-l$. While the vertically polarized sub-beam propagates clockwise and do not acquire any spatially inhomogeneous phase. Because the SLM only offers phase modulation to the horizontal polarization beam and reflects off the vertical one without vortex phase modulation. The Jones vector of the beam before the QWP2 is

$$[\cos \gamma - i \cos(2\psi - \gamma)]\text{LG}_{0,l}\hat{e}_x + [\sin \gamma - i \sin(2\psi - \gamma)]\text{LG}_{0,0}\hat{e}_y. \quad (8)$$

Then the two components pass through another quarter-wave plate (QWP2) with its optical axis inclining 45° to the horizontal direction which converts them into two orthogonal circular polarizations located on the north and south of the hybrid-order Poincaré sphere. As the Jones matrix of the quarter-wave plate can be expressed as

$$\begin{pmatrix} 1 & -i \\ -i & 1 \end{pmatrix}. \quad (9)$$

Hence, the Jones vector of the optical beam after the QWP2, i.e., the FPB based on the circular polarization eigenstates, is given by

$$[-i \sin \gamma - \sin(2\psi - \gamma)]\text{LG}_{0,0}(\hat{e}_x + i\hat{e}_y) + [\cos \gamma - i \cos(2\psi - \gamma)]\text{LG}_{0,l}(\hat{e}_x - i\hat{e}_y). \quad (10)$$

It represents the superposition of two orthogonal circular polarizations located on the north and south poles of the hybrid-order Poincaré sphere, respectively. So, we can obtain that

$$\psi_N = [-i \sin \gamma - \sin(2\psi - \gamma)], \quad \psi_S = [\cos \gamma - i \cos(2\psi - \gamma)]. \quad (11)$$

Substituting the above two equations into Eq. (5), we can establish the relationship between the generated FPBs and the two tunable parameters, γ and ψ , i.e.,

$$\tan\left(\frac{\theta}{2}\right) = \left[\frac{\cos^2 \gamma + \cos^2(2\psi - \gamma)}{\sin^2 \gamma + \sin^2(2\psi - \gamma)}\right]^{1/2}, \quad \Phi = \tan^{-1}\left[-\frac{\cos(2\psi - \gamma)}{\cos \gamma}\right] - \tan^{-1}\left[\frac{\sin \gamma}{\sin(2\psi - \gamma)}\right]. \quad (12)$$

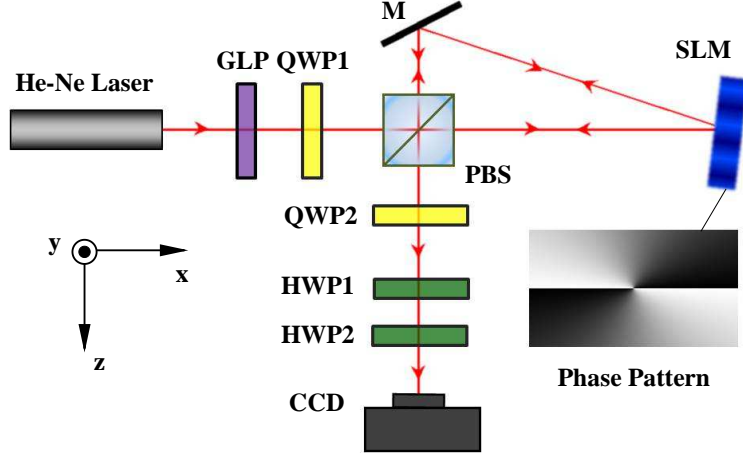


FIG. 2: Experimental setup for generating the FPs. An He-Ne laser outputs a linearly polarized light beam whose polarization state can be tuned to arbitrary linear, circular, or elliptical polarization by modulating the Glan laser polarizer (GLP) and the quarter-wave plate (QWP1). Then the beam passes through the PBS and is split into two sub-beams with the transmission beam being a horizontal polarization and the reflection beam being a vertical one. The spatial light modulator (SLM) applies a helical phase to the horizontal component and reflects off the vertical component without vortex phase modulation. The PBS, the SLM, and the Mirror (M) forms a Sagnac interferometer. Another quarter-wave plate (QWP2) converts the two sub-beams into orthogonal circular polarizations located on the north and south poles on the hybrid-order Poincaré sphere. Two cascaded half-wave plate are employed to manipulate the FPs moving along the latitude of the sphere. A CCD camera is used to record the beam intensity. The insets: a phase pattern with topological charge $l = 2$ displayed on the SLM.

In this case, any desired FPB can be generated over the hybrid-order Poincaré sphere by suitably modulating the GLP and QWP1.

In fact, $LG_{0,l}$ beam exhibits an additional phase factor $\exp[i|l|\xi(z)]$ which is z -dependent, that is, the polarization geometry of the generated FPB changes upon propagation. To compensate this phase, we employ two cascaded half-wave plates (HWP1 and HWP2) with their optical axes inclined angles ζ_1 and ζ_2 with respect to the horizontal direction, respectively. Then the Jones vector of the output beam is given by

$$\psi_N \exp[-i2(\zeta_1 - \zeta_2)] LG_{0,0}(r, z)(\hat{e}_x + i\hat{e}_y) + \psi_S^l \exp[i2(\zeta_1 - \zeta_2)] LG_{0,l}(r, z)(\hat{e}_x - i\hat{e}_y). \quad (13)$$

One finds that the two cascaded half-wave plates only apply an opposite phase factor $\exp[\pm i2(\zeta_1 - \zeta_2)]$ determined by the relative direction of optical axes of the two plates, to the two circular polarization eigenstates. From Eq. (3), one knows this only changes Φ . And θ remains

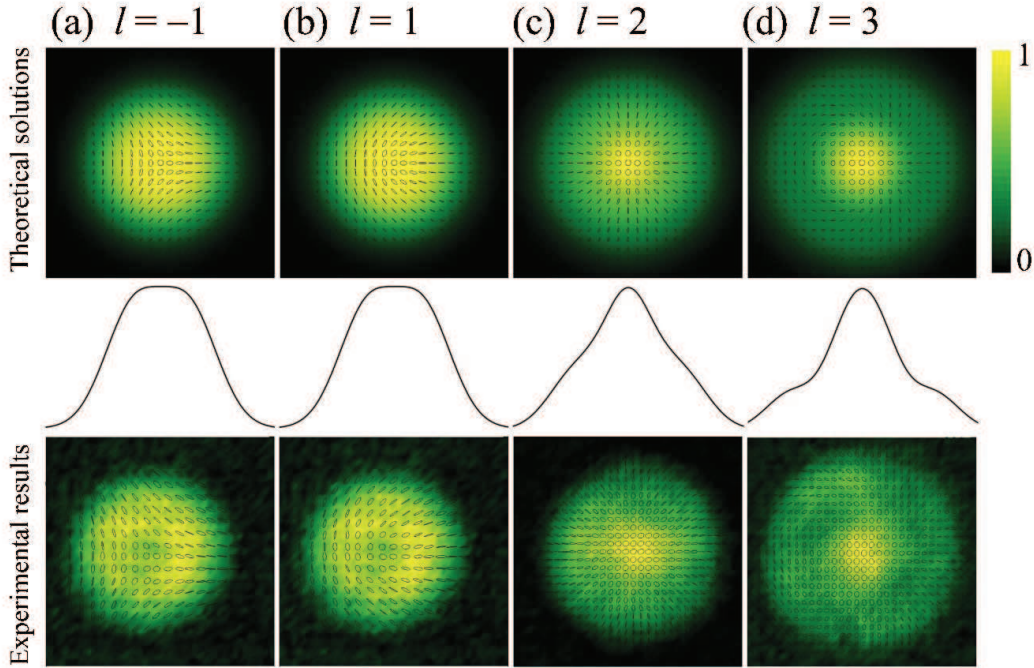


FIG. 3: Maps of the polarization states (ellipses) on the background of the intensity distribution of the FPBs for different topological charges ($l = -1, 1, 2$, and 3) under the condition of $(\theta, \Phi) = (90^\circ, 0)$. The top row depicts the theoretical solutions of the FPBs and their polarization geometries. The middle row gives the one-dimensional intensity distribution of the FPBs at $y = 0$. The bottom row is the corresponding experimental results.

unchanged. So, the two cascaded half-wave plates will provide an effective way to manipulate the FPB moving along the latitudes of the hybrid-order Poincaré sphere.

IV. RESULTS AND DISCUSSION

We have two degrees of freedom to manipulate the generated FPBs. For one thing, we can modulate the topological charge l of the sub-beams produced by the SLM via switching the phase picture displayed on the SLM. For different topological charges, there exists different hybrid-order Poincaré spheres. For another, we can obtain any desired FPBs on the hybrid-order Poincaré sphere by modulating the transmission axis direction of the GLP and the optical axis direction of the QWP1, i.e., tuning the incident state of polarization.

We first generate the FPBs for the cases of $l = -1, 1, 2$, and 3 , as depicted in Fig. 3. Different topological charges l corresponds to different hybrid-order Poincaré sphere. We set $\gamma = \pi/4$ and $\psi = 0$, so the FPBs locate on the sphere with $(\theta, \Phi) = (\pi/2, 0)$, i.e., at the S_1 on the equator. To

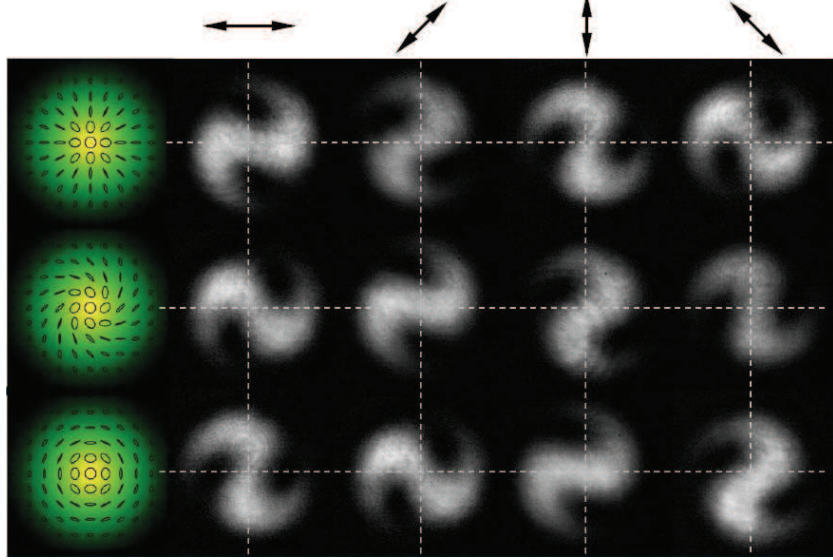


FIG. 4: CCD recorded intensity of the FPBs on the equator ($\Phi = 0, \pi/2,$ and π) after a polarizer (not shown in Fig.3) with different direction of transmission axis (represented by the arrows in the first row).

retrieve the local polarization distribution, we measure the Stokes parameters by a typical setup, a quarter-wave plate, a polarizer (not shown in the figure), and a CCD. So, the polarization state can be reconstructed pixel by pixel via solving the measured Stokes parameters. The experimental results agree with the theoretical solutions. Note that these FPBs have flattop intensity distribution, especially for $l = \pm 1$, although the polarization state is inhomogeneous. The Gaussian distribution of intensity for one eigenstate exactly offsets the doughnut-shaped $LG_{0,l}$ intensity of another eigenstate.

The local polarization state of the FPB is determined by the local amplitude and phase of the two eigenstates. Because of the circular symmetry of beam intensity in the azimuthal direction, the local amplitude ratio of the two eigenstates remains unchanged and the phase changes continuously. So the local polarization ellipse keep the same ellipticity, but varies the direction of principal axes. Obviously, the polarization pattern has a topological charge of $l/2$. In the radial direction, the local amplitude ratio varies continuously but the phase difference is a constant, so the ellipticity of the local polarization changes from left circular, through elliptical, to linear, and then to right-handed elliptical, and the direction of principal axes remains unvaried. When the amplitude ratio equal to 1, the local polarization is linear, which is associated with the L-lines singularities [16, 19]. In a word, the polarization geometry of each FPB covers all the possible state on the fundamental Poincaré sphere.

In fact, the $LG_{0,l}$ beam exhibits a z -dependent phase factor, $\exp[i|l|\xi(z)]$, which results in the

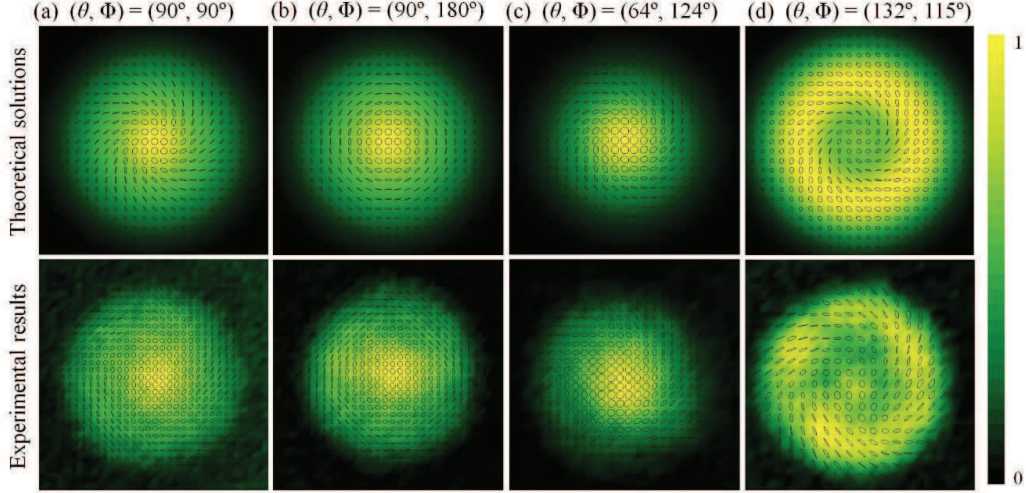


FIG. 5: Examples of the FFBs on the hybrid-order Poincaré sphere. (a) $(\theta, \Phi) = (90^\circ, 90^\circ)$. (b) $(\theta, \Phi) = (90^\circ, 180^\circ)$. (c) $(\theta, \Phi) = (64^\circ, 124^\circ)$. (d) $(\theta, \Phi) = (132^\circ, 115^\circ)$. The top row is the theoretical solutions and the bottom row is the corresponding experimental results.

variation of Φ upon beam propagation (θ remains unchanged). In other words, the FFBs will move along a latitude on the hybrid-order Poincaré sphere when they propagate in free space. To compensate this additional phase introduced by beam propagation, two cascaded half-wave plates, HWP1 and HWP2, are employed. Because the half-wave plates only influence the phase of the eigenstates, as depicted theoretically in Eq. (13). We choose three typical FFBs on the equator of the hybrid-order Poincaré sphere ($\Phi = 0, \pi/2$, and π) and analyze their polarization using a polarizer, as depicted in Fig. 4. Rotating the polarizer, the recorded intensities in the CCD camera shows “S”-shaped patterns whose rotation direction is the same as that of the polarizer. At a propagation distance ($z \neq 0$), due to the beam propagation, Φ changes continuously. By modulating the relative optical axis direction of the HWP1 and HWP2, i.e., $\zeta_1 - \zeta_2$, and rotating the polarizer, the intensity rotations depicted by Fig. 4 can be found in this process. Take any case of the three states as a reference, we can realized any other intermediate state on the equator. Further, tuning the GLP and QWP1, the FFBs can be switched to any desired latitude. Hence, any desired FFBs on the hybrid-order Poincaré sphere can be realized by the combined use of a polarizer and a quarter-wave plate controlling the incident state of polarization and two cascaded half-wave plates manipulating the phase of the eigenstates.

By solving Eq. (13), we obtain the corresponding mapping relationship between (θ, Φ) and (γ, ψ) , so the latitude of the FFB is first determined. Based on any case in Fig. 4 and tuning $\zeta_1 - \zeta_2$ to the appropriate value, we can therefore acquire the required FFBs on the hybrid-order Poincaré

sphere. FPBs located on $(\theta, \Phi) = (90^\circ, 90^\circ)$, $(90^\circ, 180^\circ)$, $(64^\circ, 124^\circ)$, and $(132^\circ, 115^\circ)$, are solved, as depicted in Fig. 5. The first and the second FPBs are on the equator, and the third FPB locates on the northern hemisphere, while the fourth one is on the southern hemisphere.

V. CONCLUSIONS

We have employed a hybrid-order Poincaré sphere to describe the FPBs, whose eigenstates are a pair of orthogonally circularly polarized Gaussian beam and Laguerre-Gaussian beam. An experimental setup has also been established to generate any desired FPBs over the hybrid-order Poincaré sphere. The combination usage of the GLP, QWP1, HWP1, and HWP2 is crucial for manipulating the FPBs. It is worth to mention that if the WQP2 is removed, the linear-polarization based FPBs can be generated [12] and the corresponding hybrid-order Poincaré sphere with its orthogonal eigenstates being linearly polarized Gaussian beam and Laguerre-Gaussian beam can also be established. Our research may provide an alternative way for describing the full Poincaré beam and an effective method to study the polarization singularities and geometric Panacharatnam-Berry phase of light [11, 16, 21, 22].

Acknowledgments

This research was partially supported by the National Natural Science Foundation of China (Grants No. 11447010), the Natural Science Foundation of Hunan Province (Grant No. 2015JJ3026), the China Postdoctoral Science Foundation (Grant No. 2014M562198), the Science Foundation of Hengyang Normal University (Grant No. 12B37), and the Construct Program of the Key Discipline in Hunan Province.

-
- [1] For example, M. Born and E. Wolf, *Principles of Optics* (University Press, Cambridge, 1997).
 - [2] D. G. Hall, "Vector-beam solutions of Maxwells wave equation," *Opt. Lett.* **21**, 9-11 (1996).
 - [3] Q. Zhan, "Cylindrical vector beams: from mathematical concepts to applications," *Adv. Opt. Photon.* **1**, 1-57 (2009) and references therein.
 - [4] A. Holleczek, A. Aiello, C. Gabriel, C. Marquardt, G. Leuchs, "Classical and quantum properties of cylindrically polarized states of light," *Opt. Express* **19**, 9714-9736 (2011).

- [5] G. Milione, H. I. Sztul, D. A. Nolan, and R. R. Alfano, “Higher-Order Poincaré Sphere, Stokes Parameters, and the Angular Momentum of Light,” *Phys. Rev. Lett.* **107**, 053601 (2011).
- [6] A. Niv, G. Biener, V. Kleiner, and E. Hasman, “Manipulation of the Pancharatnam phase in vectorial vortices,” *Opt. Express* **14**, 4208-4220 (2006).
- [7] M. Beresna, M. Gecevičius, P. G. Kazansky, and T. Gertus, “Radially polarized optical vortex converter created by femtosecond laser nanostructuring of glass,” *Appl. Phys. Lett.* **98**, 201101 (2011).
- [8] H. Chen, J. Hao, B. F. Zhang, J. Xu, J. Ding, and H. T. Wang, “Generation of vector beam with space-variant distribution of both polarization and phase,” *Opt. Lett.* **36**, 3179-3181 (2011).
- [9] Z. Zhao, J. Wang, S. Li, and A. E. Willner, “Metamaterials-based broadband generation of orbital angular momentum carrying vector beams,” *Opt. Lett.* **38**, 932-934 (2013).
- [10] X. Yi, X. Ling, Z. Zhang, X. Zhou, Y. Liu, S. Chen, H. Luo, and S. Wen, “Generation of cylindrical vector vortex beams by two cascaded metasurfaces,” *Opt. Express* **22**, 17207-17215 (2014).
- [11] X. Yi, Y. Liu, X. Ling, X. Zhou, Y. Ke, H. Luo, S. Wen, and D. Fan, “Hybrid-order Poincaré sphere,” *Phy. Rev. A* **91**, 023801 (2015).
- [12] A. Beckley, T. Brown, and M. Alonso, “Full Poincaré beams,” *Opt. Express* **18**, 10777-10785 (2010).
- [13] A. Beckley, T. Brown, and M. Alonso, “Full Poincaré beams II: partial polarization,” *Opt. Express* **20**, 9357-9362 (2012).
- [14] W. Han, W. Cheng, and Q. Zhan, “Flat-top focusing with full Poincaré beams under low numerical aperture illumination,” *Opt. Lett.* **36**, 1605-1607 (2011).
- [15] E. J. Galvez, S. Khadka, W. H. Schubert, and S. Nomoto, “Poincaré-beam patterns produced by non-separable superpositions of Laguerre-Gauss and polarization modes of light,” *Appl. Opt.* **51**, 2925-2934 (2012).
- [16] F. Cardano, E. Karimi, L. Marrucci, C. de Lisio, and E. Santamato, “Generation and dynamics of optical beams with polarization singularities,” *Opt. Express* **21**, 8815-8820 (2013).
- [17] T. Bauer, P. Banzer, E. Karimi, S. Orlov, A. Rubano, L. Marrucci, E. Santamato, R. W. Boyd, G. Leuchs, “Observation of optical polarization Möbius strips,” *Science* **347**, 964-966 (2015).
- [18] G. M. Philip, V. Kumar, Giovanni Milione, and N. K. Viswanathan, “Manifestation of the Gouy phase in vector-vortex beams,” *Opt. Lett.* **37**, 2667-2669 (2012).
- [19] V. Kumar and N. K. Viswanathan, “Topological structures in vector-vortex beam fields,” *J. Opt. Soc. Am. B* **31**, A40-A45 (2014).
- [20] E. J. Galvez, B. L. Rojec, V. Kumar, and N. K. Viswanathan, “Generation of isolated asymmetric

umbilics in light's polarization," Phys. Rev. A **89**, 031801(R) (2014).

[21] J. C. Gutiérrez-Vega, "Pancharatnam-Berry phase of optical systems," Opt. Lett. **36**, 1143-1145 (2011).

[22] V. Kumar and N. K. Viswanathan, "The Pancharatnam-Berry phase in polarization singular beams," J. Opt. **15**, 044026 (2013).